Volume 1, Issue 1, pp 53 - 69, year 2024

Journal of the Egyptian Society for Basic Sciences-Physics (JESBSP)
https://jesbsp.journals.ekb.eg/

Mid-, and long-term periodicities of interplanetary plasma parameters throughout the period (1967-2017): Case Study, the distribution of hemispheric solar activities by using the wavelet analysis

El-Taher[1] A M, El-Borie[2] M A, Ibrahim[1] S F, and Elsayed A Tayel [2]

[1] Physics and Chemistry Dept., Faculty of Education, Alexandria University, Alexandria, Egypt. [2] Physics Dept., Faculty of Science, Alexandria University, Alexandria, Egypt.
Corresponding author: amreltaher@alexu.edu.eg

Abstract

In this article, mid-, and long-term periodicities of interplanetary plasma parameters (*B*, *V*, *n*, *T*, and *P*) aaccording to the distribution of the hemispheric *SSAs* in solar hemispheres utilizing the wavelet analysis throughout the period 1967-2017 have been examined. The association between the *SSAs* and each interplanetary plasma parameter can be established if and only if both the *SSAs* and the daily averages of each interplanetary plasma parameter have been smoothed by a window of a 3-year running average and a particular time-lag has been applied. The solar activity cycle (~ 10.7 yr), that has almost same power, is the most prominent periodicity in B_N and B_S power spectra. In addition, the wavelet power spectra of SWS_N and SWS_S displayed a broad variety of periodicities and their temporal evolutions. The GWS of SWS_S provided two significant peaks at 9.8 and 15.2-yr, as well as at 13.9- yr, for SWS_N. Furthermore, the most prominent peaks are the periodicities at 9.8 and 13.9 years (9.8 and 15.2 years) for T_N (T_S) spectra. Additionally, the periodicity around 1.5-yr reveals an increase in power throughout the time intervals (1968-1976) and (1982-1987) for T_N and (1970-1972), (1975-1983), and (1985-1993) for T_S.

Keywords: solar wind parameters, interplanteraty magnetic fileld, Wavelet power spectra, hemispheric sunspot areas

Declarations The authors have no relevant financial or non-financial interests to disclose.

1. Introduction

The sun's magnetic activity cycle is an almost periodic 11-year fluctuations in the Sun's activity as measured by variations in sunspots on the solar surface. Solar flares, prominences, coronal mass ejections (CMEs), high-speed solar wind, and solar energetic particles are all characteristics of solar activity. All solar activity is driven by the sun's magnetic field. Increased solar energy results in variations in intense ultraviolet and X-rays, which have a significant influence on the Earth's upper atmosphere. Solar flares, prominences, coronal mass ejections (CMEs), high-speed solar wind, and solar energetic particles are all characteristics of solar activity. All solar activity is driven by the sun's magnetic field. Increased solar activity results in variations in intense ultraviolet and X-rays, which have a significant influence on the Earth's upper atmosphere. The solar cycle is naturally magnetic in nature and is created by dynamo mechanisms in the Sun (see [1] for a review of the solar dynamo). Although it is difficult to ascertain how, when, and where dynamo processes operate, several fundamental dynamo features are sufficiently widely accepted and provide a framework for explaining solar-cycle activities. Solar activity is the most remarkable aspect of the solar disc, which may be characterized by sunspot numbers (*SSNs*) or sunspot regions (*SSAs*). The comparison of the revised *SSAs* with the international *SSNs* indicated that both solar activity quantities are indeed highly correlated, the correlation coefficient = 0.994 [2]. There is no evidence that the two quantities are either in lead or in lag during the solar cycle. Moreover, except for one aspect, at the zero point, both quantities could be used interchangeably. On the other hand, the north-south (N-S) asymmetry for different solar activity indcies has been investigated; such as *SSNs* [3], *SSAs* [3]–[8], sunspot groups [7], [9], solar flares [10], Hα flare indices [3], [9], [11]–[13], solar active prominences [9], [14], [15], coronal mass ejections [3], [16], soft X-ray flares [17], [18], the geomagnetic activity indcies and solar wind parameters [20]–[25]and the magnetic fluxes [3], [25].

A database of hemispheric *SSNs* (northern and southern *SSNs*) spanning the time interval 1945–2004 was constructed by [26]. [7] investigated the asymmetry of solar activity from 5/1996 to 2/2007 using sunspot groups and *SSAs*. For solar cycle 23, their findings revealed that solar activity was more pronounced in the southern solar hemisphere than in the northern one. [23] investigated the asymmerty of solar (*SSNs* and solar radio flux *SF*) and interplanertary plasma parameters (interplanetary magnetic field magnitude (IMF) *B*, solar wind speed *SWS*, plasma density *n*, plasma dynamic pressure *P*, and plasma temperature *T*) based on the IMF polarity sense (toward or away) over a period of 50 years (1967–2016). Throughout the toward polarity

days, the solar plasma was hotter than that of away polarity days during solar cycles 21 and 22. In contrast, the solar plasma was cooler and of less speed (~ 17.5 km/s) during toward than away polarity days during solar activity cycles 20 and 23. Moreover, for the time interval 1973−1993 (covering solar cycles 21 and 22).

The influence of the IMF polarity states (i.e, toward, *T* and away, *A*) on the monthly averages of *B*, *V*, and *SSNs*, as well as *aa*, *Kp*, and *Ap* geomagnetic indices over the period 1967–2016 has been studied utilizing a wavelet analysis [27]. Based on the IMF polarity states, the daily data were classified into two categories (*T* or *A*) and the monthly average of the T and A groups was calculated for each parameter. The results indicated that the wavelet power spectra (WPS) for both B_T and B_A were nearly symmetrical. The WPS for B_T and B_A displayed contributions of periodicities at 3.2–3.5, 10.7, and 18.3 yr. In addition, the WPS of V_T and V_A revealed a wide range of periodicities with their temporal evolutions. The global wavelet spectrum (GWS) for V_A showed two prominent peaks (within the 95% confidence level) at 9.8 and 15.2 yr, as well as at 1 and 9.8 year for V_T. Furthermore, for the V_T spectrum, the presence of 1 yr periodicity was obvious and it was shifted to 1.5 yr in the case of V_A spectrum. The absence of the most pronounced patterns of the solar activity cycle (the 10.7 yr) and the solar magnetic cycle, the Hale cycle (22 yr), was a V_T and V_A spectra.

The daily averages of interplanetary plasma parameters (*V*, *n*, IMF magnitude *B*, and its components, *By* and *Bz*), during the 1964−2000 epoch have been investigated, using the Morlet wavelet and both associated spectra WPS and GWS [28]. They confirmed a number of prominent periodicities are present in the GWS of solar wind parameters in the range from 16 years to a few days. In the *V*, *n*, and *By*-component of IMF, the signature of global solar oscillation of ~16 yr was present. Recently, [9] studied the influence of the distribution of the monthly averages of the hemispheric *SSAs* for some solar indices (the solar radio flux *F10.7*, the plage area *PA*, the coronal index *CI*, the solar mean magnetic field *B*, and the solar flare index *SFI*). Their study indicated that, excluding *B*, the solar activity cycle (~10.7 years) is the most prevalent period (above the 95% confidence levels) in both the WPS and GWS for both hemisphere groups over the entire timeframe. Other identified periods were found to be insignificant in comparison to the 10.7-year periodicity, having less relevance (below the 95 % confidence level). The most notable characteristic for *B* is the absence of the pronounced peak of the solar activity cycle. The Hale cycle is clearly noticeable in both hemispheric groups of *B*, with a slight time shift between them. The significance of short- and mid-term periodicities of solar indices has been also identified and introduced by using the moving average method which performed previously [29]–[32].

In the present work, we utilize the continuous wavelet power spectrum to investigate the periodicities for the northern and southern groups of interplanetary plasma parameters (the IMF magnitude B, plasma velocity V, plasma density n, plasma dynamic pressure P, and plasma temperature T) during the time interval 1967–2017. Long- and intermediate-term oscillations have been identified using the monthly averages of each considered interplanetary plasma parameters. Furthermore, possible temporal changes over the considered interplanetary plasma parameters have been examined, applying the wavelet approach.

2. Data Resources and Analysis

Basically, we used different kinds of interplanetary plasma parameters related to the solar activities as the followings:

a- The monthly averages of hemispheric measurements of *SSAs* during the period 1/1967-12/2017 which were taken via: <http://solarcyclescience.com/activeregions.html>.

b- Daily averages for interplanetary plasma parameters (B, n, V, P, and T) throughout the time interval 1967−2017, which were provided by < http://omniweb.gsfc.nasa.gov/form/dx1.html>.

To investigate the influence of solar activity (represented by *SSAs*) on the interplanetary plasma parameters, a smoothing window of a 3-yr running average of the daily averages of both *SSAs* and interplanetary plasma parameters as well as a specific time-lag of 3-yr (between *SSAs* and each of T, V, and P) and 2-yr (between *SSAs*&n) should be taken into our consideration [33]. The monthly averages of each interplanetary plasma parameter have been classified into two groups, northern (N) and southern (S), according to the monthly averages of hemispheric distribution of *SSAs* in solar hemispheres. B_N (B_S), V_N (V_S), n_N (n_S), P_N (P_S), and T_N (T_S) refer to the monthly averages of N (S) hemispheric groups for B, V, n, P, and T, respectively. The monthly average of each hemispheric group for each parameter has been smoothed by seven-month moving average window then the obtained smoothed data of N and S groups were analyzed using the wavelet technique.

Periodicities may be extracted from a time series using many approaches, including the fast Fourier transform (FFT), the maximum entropy method (MEM), and the Morlet wavelet transform (WT). The wavelet transform is a mathematical technique that is commonly utilized in signal processing applications. It has the ability to decompose particular patterns hidden in large amounts of data. The wavelet transform may display functions and reveal their local features in the time-frequency domain at the same time. The WT is suitable for investigation of a time series containing nonstationary power at many different frequencies as its functions (wavelets) are localized in both time and frequency domains [34]–[36]. In comparison to other

period investigation procedures, the Morlet WT technique is the better one. It permits evaluating possible temporal variations of the oscillations detected in any time series. It is additionally an efficient way for determining hidden periodicities in time series. Unlike the FFT, the WT detects not only the fundamental scales (frequencies) of periodicities, but also their localization on the time axis [37]. In general, wavelets are localized in both time and frequency, whereas typical Fourier transforms are simply localized in frequency. According to [36], The discrete wavelet transform of a signal x_n can be written in the following form:

$$W_k(s) = \sum_{n=0}^{N-1} X_n \psi^* \left[\frac{(k-n)\delta t}{s}\right], \quad (1)$$

where $W_k(s)$ are the wavelet transform coefficients, s is the scale, k is the shift along the time axis, δt is the time period between the adjacent measurements, and ψ is the wavelet function. Instead of Equation (1), the equivalent expression can be written as follows:

$$W_k(s) = \sum_{n}^{N-1} \hat{X}_n \hat{\psi}^*(sw_n) e^{iw_n k}, \quad (2)$$

where $\psi^*(sw_n) = \left(\frac{2\pi s}{\delta t}\right)^{1/2} . \hat{\psi}_0(sw_n)$ and $\int_{-\infty}^{\infty} |\psi(\acute{\omega})|^2 d\acute{\omega} = 1$, whereas N is the number of points in the time series, and ψ_0 is the basic wavelet function for which we took the Morlet wavelet that localized in the time and frequency domains. Here, η is a dimensionless parameter:

$$\psi_0(\eta) = \pi^{-1/4} e^{i\omega_0 \eta} . e^{(-\eta^2/2)}$$

here, ω_0 is a non-dimensional frequency, which was taken to be equal to 12 for midterm frequency ranges and $\omega_0 = 6$ for low frequency ranges [37].

3. Results and Discussions

Figures 1-5 display the periodograms of temporal evolution of the WPS and GWS for the interplanetary plasma parameters *B*, *V*, *T*, *n*, and *P*, respectively. The WPS (GWS) of the time series is displayed in the left (right) panels. The top (bottom) plots of each Figure represent the northern (southern) hemispheric group of the monthly averages, for each plasma solar parameter based on the hemispheric distributions of *SSAs*. The y-axis in the WPS represents the periodicity in years, while the x-axis indicates the timeframe of data observation. In addition, information on the contours can clarify the spectral power levels that are appropriate to each variation at various times. The thick (black line) contour is the 95 % confidence level

in the spectrum region. The GWS (right plot) shows the change in power over its period and the thick dashed line is the 95 % confidence level. Tables 1 and 2 list the GWS and WPS periodicities of the northern and southern groups of the monthly averages for B, V, n, P, and T, respectively, based on the hemispheric distribution of *SSAs* over the period 1967−2017. The powers of the observed periodicities and their time periods are also tabulated.

Figure 1 shows the WPS and the corresponding GWS of monthly averages of B for B_N (plots a &b) and B_S (plots c&d) over the period 1967–2017. It can be seen both B_N and B_S reveal a long-term periodicity (the solar activity cycle at 11.7 yr) with nearly the same magnitude of power. Also, the WPS of B_N and B_S shows a common periodicity in the range 1–2 yr during the periods 1981−1986 and 1990−1994 for B_N and 1975−1980 and 2012−2014 for B_S. Furthermore, the two plots show an increase of power in the frequency range 2–4 yr during the timespan 1973−1986, 2005−2009 for B_N and 1986–1995 for B_S. For the B_N and B_S spectra, the observed periods involve quasi-biennial (2.5 yr) and quasi-triennial (3.8 yr) oscillations, respectively. The GWS of B_N reflects a periodicity around 5.4 yr (it may be the 2nd harmonic of 11-yr solar activity cycle) while a periodicity of ~ 1.7 yr (a tiny periodicity) is noted in B_S spectrum. We have to not that the study of [38] confirmed the occurrence of 1.7 yr periodicity in cosmic rays for solar cycle 21. Also, [39] showed the ~1.7-year quasi-periodic variation of cosmic ray intensity is connected to the Sun's energy release via solar activity to the IMF. These periodicities were identified before for several interplanetary plasma parameters ([40]–[42] , and references therein). Moreover, a variation of 18-yr oscillation has been observed during the entire period for both B_N and B_S spectra. Finally, a careful study of the wavelet spectrum for B_N and B_S shows that there is a contribution of some periodicities at 1.7-2.5-, 11.7-, and 18-yr variations, indicating that both the WPS for B_N and B_S have nearly symmetrical power spectra.

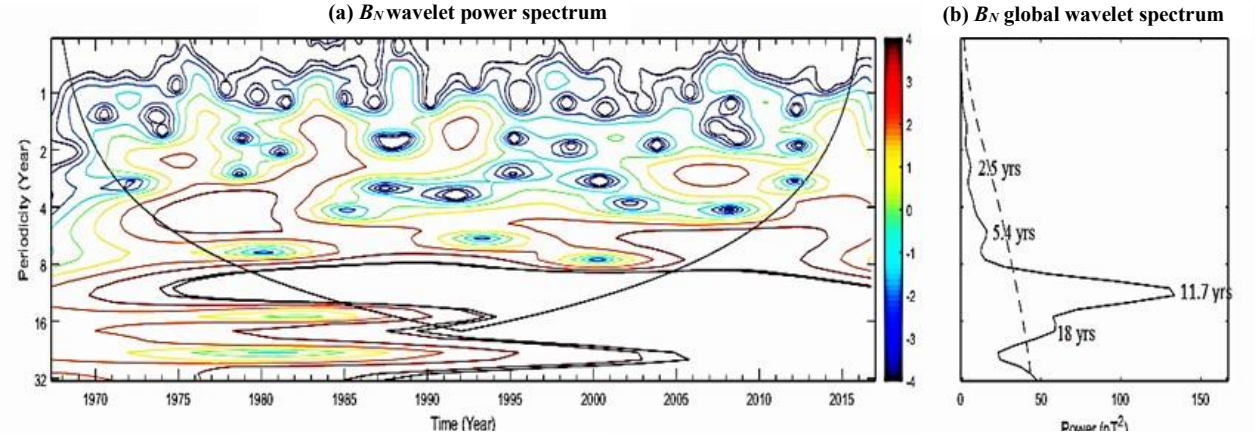

(a) B_N wavelet power spectrum (b) B_N global wavelet spectrum

(c) B_S wavelet power spectrum (d) B_S global wavelet

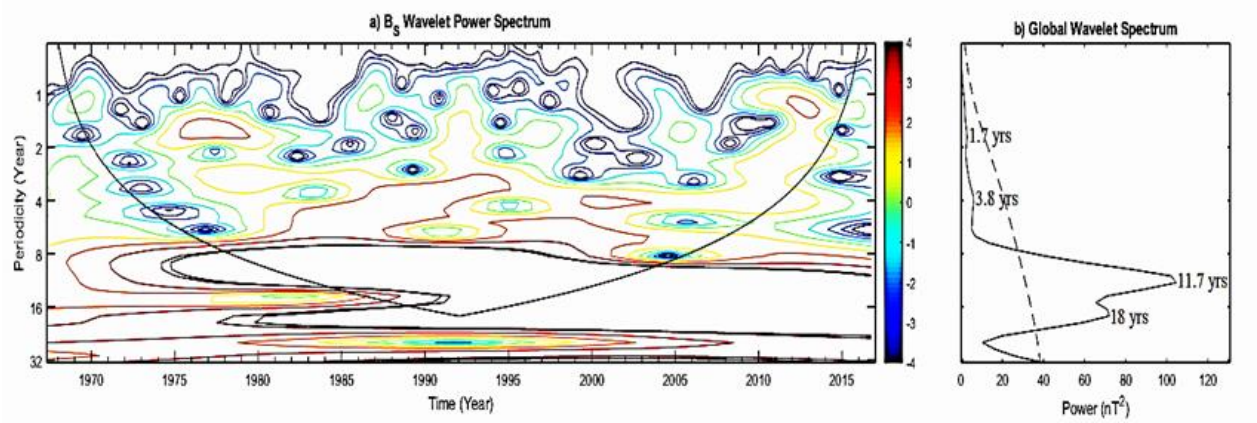

Figure 1. Wavelet spectra of the monthly averages for B_N (plots a&b) and B_S (plots c&d) based on the distribution of hemispheric *SSAs* during the period 1967-2017

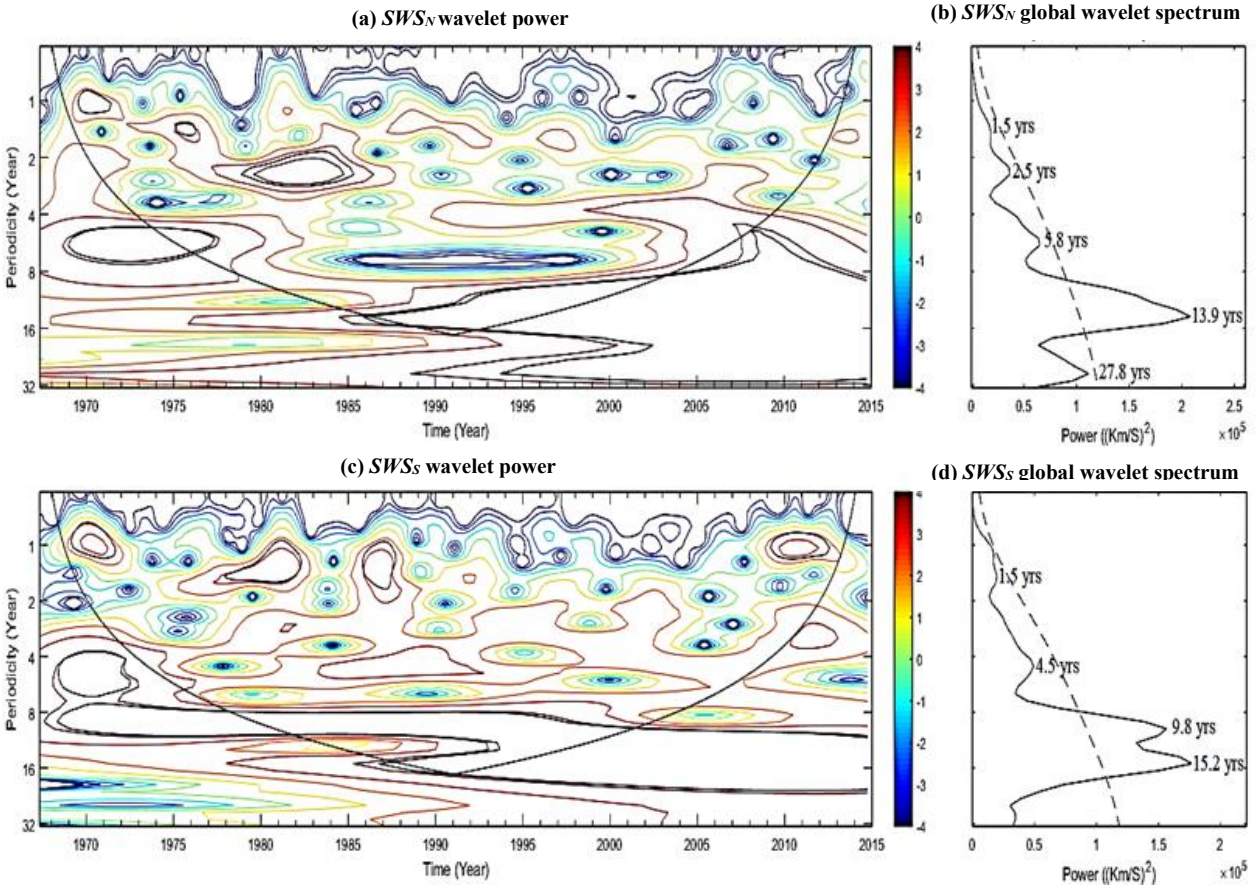

Figure 2. Same as Figure 1 for SWS_N (plots a&b) and SWS_S (plots c&d).

Figure 2 displays the WPS and GWS for solar wind speed (*SWS*) according to the distribution of hemispheric *SSAs*. The WPS and GWS for the northern and southern of solar wind speed groups (SWS_N and SWS_S) are shown in plots a&b and c&d, respectively. The contours of WPS of SWS_N and SWS_S displayed a broad variety of periodicities and their temporal evolutions. The solar wind speed groups nearly display different spectra. The GWS of SWS_S reveals two prominent peaks (within the 95 % confidence level) at 9.8 and 15.2-year, as well as 13.9 yr for

SWS_N. Both spectra of *SWS* groups reflect a common peak around 1.5 yr below the 95%

Table 1. Wavelet power spectra periodicities for *B*, *V*, and *T* (for the northern and southern hemispheric groups), based on the distribution of hemispheric *SSAs* over the period 1967–2017

Parameter	group	GWP Periodicity	Power	WPS (95 % C.L)	Time Periods
B	B_N	2.5-yr 5.4-yr 11.7-yr 18-yr	6.19 16.31 133.7 58.91	1-2 yr 2-4 yr 4-8 yr 8-16 yr	(1981-1986), (1990-1994) (1973-1986), (2005-2009) (1972-2014) During the whole interval
	B_S	1.7-yr 3.8-yr 11.7-yr 18-yr	2.83 5.89 104.6 72.02	1-2 yr 2-4 yr 4-8 yr 8-16 yr	(1975-1980), (2012-2014) (1986-1995) (1973-2003) During the whole interval
SWS	SWS_N	1.5-yr 2.5-yr 5.8-yr 13.9-yr 27.8-yr	$1.8*10^4$ $3.6*10^4$ $6.5*10^4$ $2.1*10^5$ $1.1*10^5$	1-2 yr 2-4 yr 4-8 yr 8-16 yr	(1969-1998) (1975-1988), (1998-2009) (1967-1982), (1990-2015) During the whole interval
	SWS_S	1.5-yr 4.5-yr 9.8-yr 15.2-yr	$2*10^4$ $4.9*10^4$ $1.6*10^5$ $1.8*10^5$	1-2 yr 2-4 yr 4-8 yr 8-16 yr	(1969-1972), (1975-1983), (1985-1989), (2009-2013) (1978-2015) (1967-1993) During the whole interval
T	T_N	1.5-yr 4.1-yr 9.8-yr 13.9-yr	$2.8*10^9$ $9*10^9$ $3.5*10^{10}$ $6*10^{10}$	1-2 yr 2-4 yr 4-8 yr 8-16 yr	(1968-1976), (1982-1987) (1977-1985) (1990-2013) During the whole interval
	T_S	1.6-yr 2.5-yr 4.9-yr 9.8-yr 15.2-yr	$3.8*10^9$ $4.3*10^9$ $9*10^9$ $4.4*10^{10}$ $4.6*10^{10}$	1-2 yr 2-4 yr 4-8 yr 8-16 yr	(1970-1972), (1975-1983), (1985-1993) (1988-2006) (1967-2012) During the whole interval

confidence level. Furthermore, it can be shown that the spectral power of SWS_N achieves a maximum at a periodicity of 13.9 yr over the whole period within the 95 % confidence level, as well as at periods of 9.8 and 15.2 yr for SWS_S. The most obvious indicator is the absence of the most significant peak of solar activity (the 10.7 yr peak). By referring to Table 1, the strength of the 1–2-year oscillation

reaches nearly maximum possible power during 1969–1998 for SWS_N and 1969–1972, 1975, 1983, 1985, 1989, and 2009–2013 for SWS_S. Furthermore, the 2.5 and 5.8 yr oscillations for

SWS_N, are recognized, with the greatest power of the 5.8 yr period occurring between 1967 and 1982 and 1990 and 2015, within the COI. In addition, the spectral powers of SWS_N and SWS_S have a great magnitude during the frequency range 8–16 yr throughout the entire period (see Table 1). The existence of periodicities in the solar-terrestrial parameters was investigated utilizing the GWS to study their temporal behavior.

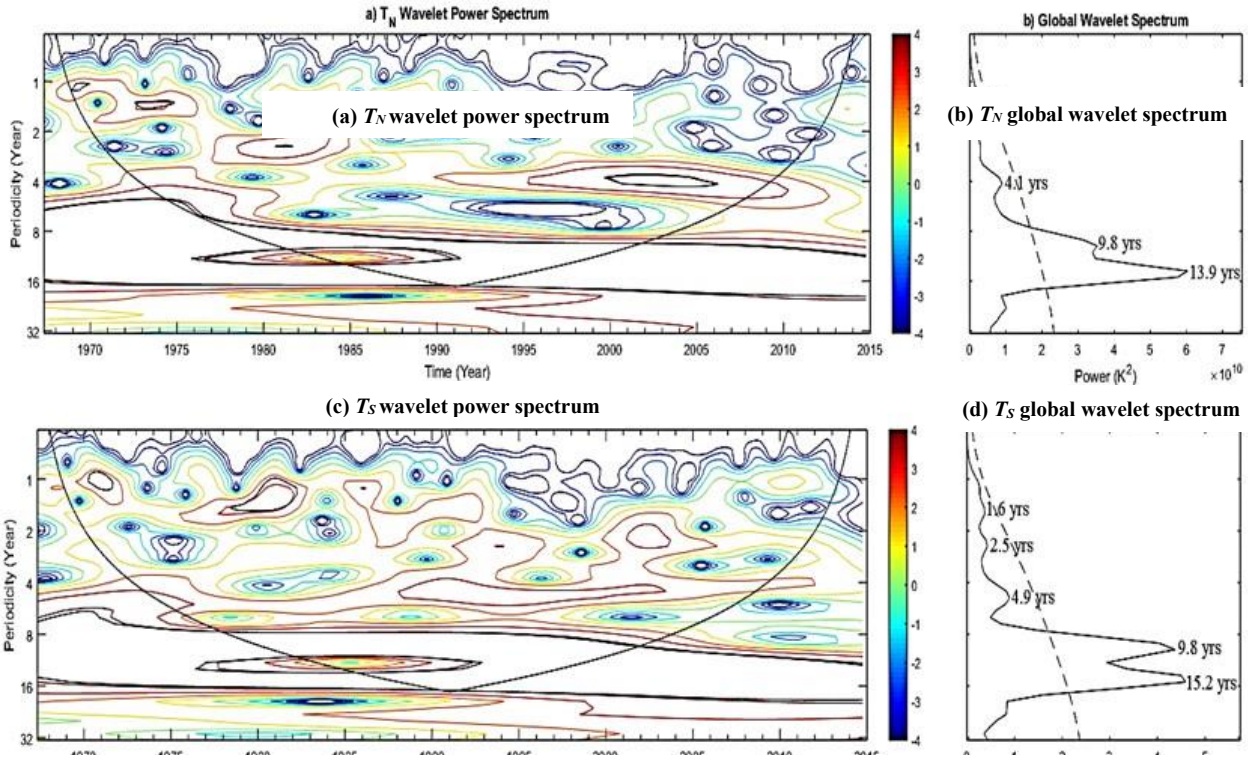

Table 1. Wavelet power spectra periodicities for *B*, *V*, and *T* (for the northern and southern hemispheric groups), based on the distribution of hemispheric *SSAs* over the period 1967−2017

Figure 3 illustrates the WPS and GWS for T_N and T_S, of monthly averages of plasma temperature (*T*) during the considered period 1967–2017. The wavelet analysis of plasma temperature (*T*) reveals that the period 8–16 yr has a significant power over the whole period for both hemispheric groups.

Table 2. GWS and WPS periodicities for *n* and *P* (for the northern and southern hemispheric groups), based on the distribution of hemispheric *SSAs* over the period 1967−201

Parameter	group	GWP Periodicity	Power	WPS (95 % C.L)	Time Periods
n	n_N	2.1-yr 4.9-yr 12.8-yr 21.4-yr	14.9 22.61 43.57 68.51	1-2 yr 2-4 yr 4-8 yr 8-16 yr	(1970-1971), (1975-1995) (1972-1993), (2001-2008) (1968-1973), (2003-2013) (1968-1989), (1999-2015)
	n_S	3.2-yr 10.7-yr 13.9-yr 21.4-yr	15.87 50.64 43.89 23.97	1-2 yr 2-4 yr 4-8 yr 8-16 yr	(1968-1972), (1976-1983), (2011-2014) (1981-1999), (2001-2013) (1971-1999) During the whole interval
P	P_N	13.5-yr 41.7-yr	14.77 54.77	1-2 yr 2-4 yr 4-8yr 8-16 yr	(1967-1970), (1987-1989) (1971-1987), (2001-2005) (1988-1993) During the whole interval
	P_S	9.6-yr 41.7-yr	19.82 63.66	1-2 yr 2-4 yr 4-8 yr 8-16 yr	(1979-1983), (1986-1989) (1984-1991) (1979-1994) During the whole interval

Also, the most prominent peaks above the COI are the periodicities at 9.8 and 13.9 years (9.8 and 15.2 years) for T_N (T_S) spectra. The main feature of the WPS for both hemispheric groups is the appearance of a double-peak structure with different location. The periodicity around 1.5 yr (corresponding to the range 1-2 yr) reveals an increase in power during the time intervals (1968-1976) and (1982-1987) for T_N and (1970-1972), (1975-1983), and (1985-1993) for T_S. A

quasi-biennial oscillation (at 2.5 yr) appears below the 95% confidence level for the GWS of the southern group of plasma temperature. Furthermore, there is a noticeable increase in period of 4–8 yr (which relates to the 4.1–4.9 yr periodicity for T_N and T_S) throughout the periods 1990-2013 and 1967-2012 compared to the other times for T_N and T_S, respectively.

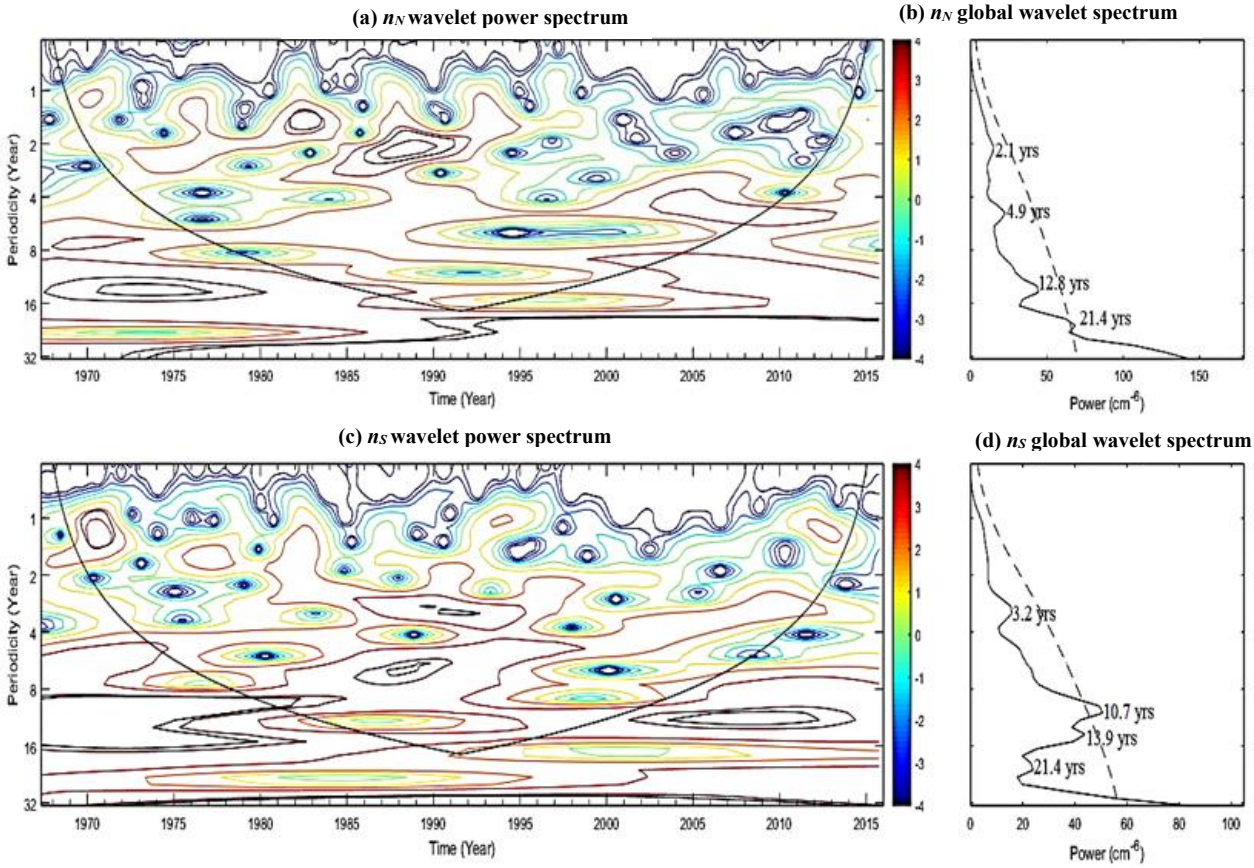

Figure 4. Same as Figure 1 for n_N (plots a&b) and n_S (plots c&d).

The WPS and corresponding GWS of monthly averages for the northern and southern groups of plasma density during the considered period are displayed in Figure 4. For the southern group (n_S) of plasma density, the well-known 10.7-year periodicity oscillation is dominating. It can be seen that this variation is pronounced throughout the whole period. A periodicity around 13.9 yr appeared just below the 95% confidence level. In the GWS of n_S, there are two signatures of smaller amplitudes, one mid- term corresponds to 3.2 yr and other of long-term at 21.4 year. The distribution of powers between these two variations within the WPS is not strong, as both power peaks are below the 95 % confidence level, but their signatures are distributed in the power spectrum. [43] studied the 22-year periodicity of direct sunspot observations over a period of around 400 years. Their findings confirmed that the 22-year periodicity (the well-known Hale cycle periodicity) is naturally generated by the 22-year magnetic dynamo cycle in the presence of a relic magnetic field. Accordingly, a consistent 22-year cycle of sunspot activity is, thus, an indication that such a magnetic relic field is present

in the Sun. Additional periodicities at 2.1-, 4.9-, and 12.8- yr exist in the GWS of the northern hemispheric group (n_N) of the plasma density.

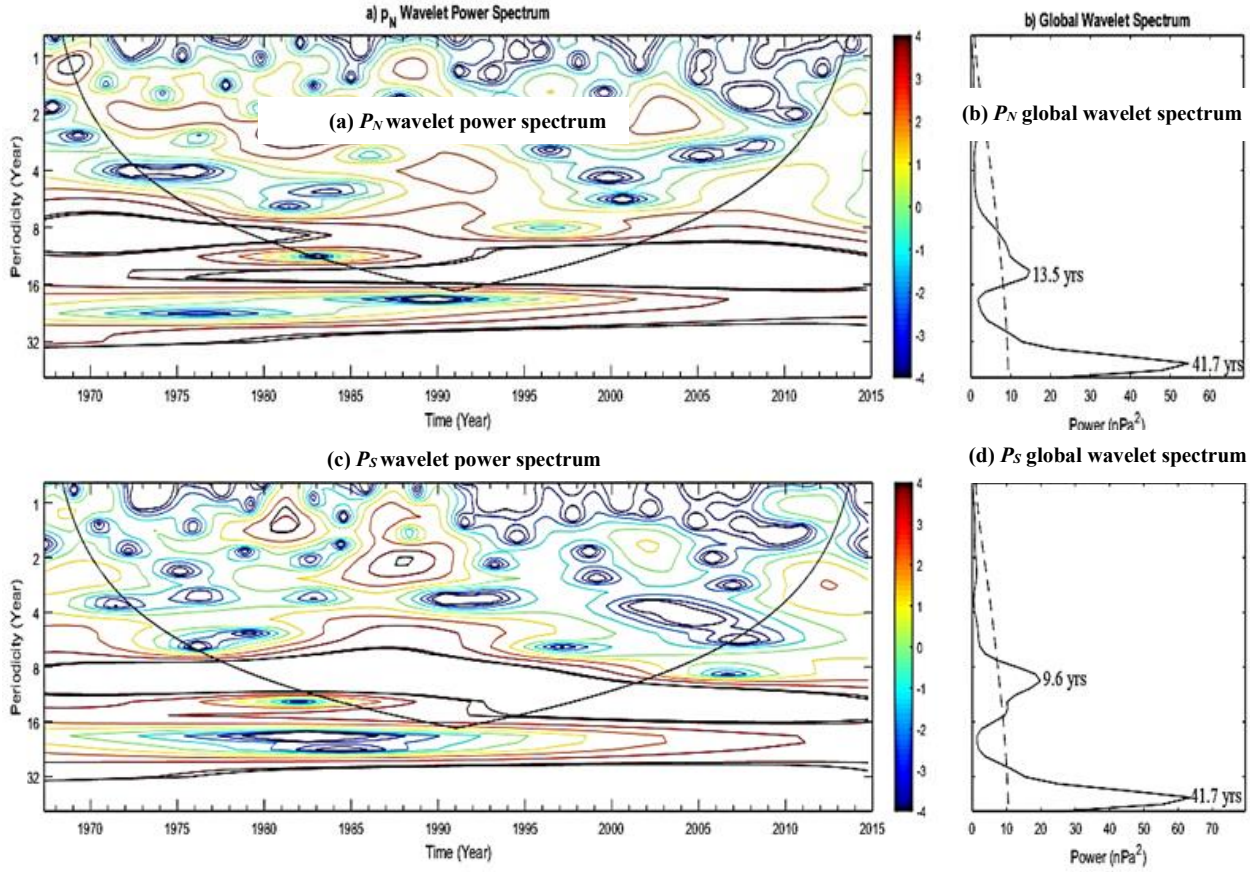

Figure 5. Same as Figure 1 for P_N (plots a&b) and P_S (plots c&d).

The wavelet power spectra of monthly averages for the northern and southern groups of plasma dynamic pressure are shown in Figure 5. The GWS reveals only prominent long-term periodicities above the 95% confidence level at 9.6- and 13.9-yr for the southern and northern groups of the plasma dynamic pressure, respectively. Also, the hemispheric groups of plasma dynamic pressure share a common long-periodicity at 41.7-yr. In addition, the WPS of the hemispheric groups of the plasma dynamic pressure shows significant power in the range 8-16 yr during the entire period. The mid-term periodicities (in the range 1-2 yr) appear through the ranges 1967−1970 and 1987−1989 for $P_{N,}$ and 1979−1983, 1986−1989 for P_S. In addition, P_N and P_S components share a periodicity in the range 2−4 yr during the intervals 1971-1987 and 2001-2005 for P_N and 1984-1991 in the case of P_S. [44] used the wavelet analysis and the Lomb/Scargle periodograms.

to investigate the prominent short-, mid-, and long- term periodicities in the solar wind parameters (V, T, n, and P), the interplanetary magnetic field (Bx, By, Bz, β, and Alfvén Mach number), and the geomagnetic activity indices (D_{ST}, AE, Ap, and Kp) throughout the time interval 1966-2010, covering four solar activity cycles. Long-term periodicities (1024-2048

days) were observed in solar wind speeds between 1972 - 1999, plasma temperature between 1972 - 2000, plasma density between 1984 - 2004 (with a peak at 4.1 years), plasma dynamic pressure between 1973 - 1995, and IMF magnitude B (1024-2048 days) during the time interval 1974 - 2000. Also, *SWS*, *T*, and *n* demonstrated mid-term periodicities (256 – 512 days with a peak at 314 days) in the time intervals 1970-1977 and 1985-1992. During the rising and maximum phases of solar cycles 20, 22, and 23, periodicities of 512-1024 days (peak at 1.7 years) have been observed in *SWS*. Also, the considered peaks were recorded (below the confidence level) in plasma temperature (peak at 2.4 years) during solar cycles 22 and 23, as well as in plasma pressure (peak at 528 days). Mid-term periodicities (256-1024 days appearing at 1.2 years) arise in the case of IMF magnitude *B* over the time interval 1987-1993, around the maximum of the solar cycle 22.

4. Conclusions

By using the wavelet technique analysis, the symmetry and/or asymmetry between the northern and southern hemispheric groups of solar wind parameters (*V*, *T*, *n*, and *P*) and the IMF magnitude *B* according to the distribution of the hemispheric *SSAs*, have been revealed by comparing their observed periodicities during the period 1967–2017. The monthly averages for the considered parameters have been separated into two hemispheric groups, northern and southern, according to the distribution of monthly averages of *SSAs*. Our findings can be summarized as follows:

i) The most prominent periodicity in B_N and B_S power spectra is the solar activity cycle of 11.7-yr with nearly the same magnitude of power. Also, the WPS of B_N and B_S showed a common periodicity in ranges 1–2 yr and 2-4 yr during different time intervals. A quasi-biennial (~ 2.5-yr) and a quasi-triennial (~ 3.8-yr) oscillations for B_N and B_S spectra, have been observed. In addition, the GWS of B_N reflects a periodicity around 5.4 yr (may be the 2 nd harmonic of 11-yr solar activity cycle) while a periodicity around 1.7 yr (appeared as a tiny periodicity) is found in B_S spectrum.

ii) The wavelet power spectra of SWS_N and SWS_S displayed a broad variety of periodicities and their temporal evolutions. The GWS of SWS_S reveals two prominent peaks (within the 95 % confidence level) at 9.8 and 15.2-year, as well as 13.9 yr for SWS_N. Both spectra of *SWS* groups reflect a common peak around 1.5 yr below the 95% confidence level. the spectral power of SWS_N achieves a maximum at a periodicity of 13.9 yr over the whole period within the 95 % confidence level, as well as at periods of 9.8 and 15.2 yr for SWS_S. The most obvious indicator is the absence of the most significant peak of solar activity (the 10.7 yr peak). The FFT analysis

for the solar wind speed measurements taken near 1 AU, have been examined during the period 1973–2000 [46]. The spectrum revealed remarkable peaks at the wavelengths 0.5-, 0.7-, 1.0-, 1.3-, and 9.6 yr. The findings verified that the 9.6-year periodicity is unrelated to the well-known periodicity of the solar activity cycle, since the only significant signature in the solar power spectrum is the 11-year (the standard solar cycle). The time difference is 1.4 years. As a result, we may conclude that the observed peak of 9.8 years appeared in SWS_S spectrum is not attributed to such 11-year oscillations.

There is no proof of a connection between the two. One hypothesis is that the reported period of 9.8 years in the in SWS_S spectrum is connected to the formation rate and the magnetic structure of active regions in the southern solar hemisphere. On the other hand, the study of [30] showed peaks around 9.6 years and 16 years in the GWS of the solar wind speed during the timespan (1964-2000) but they located outside the cone of influence in the wavelet spectrum due to the limited data length.

iii) The GWS of T_N and T_S have great power during the whole entire period during the frequency range of 8–16 yr. Also, the most prominent peaks above the COI are the periodicities at 9.8 and 13.9 years (9.8 and 15.2 years) for T_N (T_S) spectra. The main feature of the WPS for northern and southern groups is the appearance of a double-peak structure with different locations. The periodicity around 1.5 yr (corresponding to the range 1-2 yr) reveals an increase in power during the time intervals (1968-1976) and (1982-1987) for T_N and (1970-1972), (1975-1983), and (1985-1993) for T_S. Additionally, there is an obvious increase in power during the frequency range 4–8 yr (which refers to the 4.1–4.9 yr periodicity for T_N and T_S) throughout the periods 1990-2013 and 1967-2012 compared to the other times for T_N and T_S, respectively. Periodicities of 4, 8 and 11.4 years for daily measurements of plasma temperature during the time interval 1966-2010 have been identified [46]. Solar wind speed and temperature are expected to be correlated (the higher plasma temperature, the greater velocity of plasma particles). Actually, they share some common periodicities in the obtained results.

iv) The well-known 10.7-year periodicity is the dominant variation in the southern group (n_S) of plasma density during the entire period. A periodicity around 13.9 yr appeared just below the 95% confidence level. The GWS of n_S, displayed two signatures of smaller amplitude, one mid- term corresponds to 3.2 yr and other long-term at 21.4 year. The distribution of powers between these two variations within the WPS is not strong enough, as both power peaks are below the 95% confidence level.

v) The GWS of the southern and northern groups of the plasma dynamic pressure reveals only prominent long-term periodicities above the 95% confidence level at 9.6- and 13.9-yr,

respectively. Long-term periodicities have been identified at 4.9, 6.6, 8.3, and 11.8 years for the daily measurements of plasma dynamic pressure using the Lomb/Scargle periodogram method [45].

Acknowledgments

The authors are thankful to the OMNI database from the National Space Science Data Centre and The Royal Greenwich for providing the data.

References

[1] Charbonneau P, *Living Reviews in Solar Physics* **7,** p 1, 2010.

[2] Hathaway D H, *Living Reviews in Solar Physics* **12,** p 4, 2015.

[3] Ataç T and Özgüç A, *Solar Physics* **233,** p 139, 2006.

[4] Oliver R and Ballester J L *Solar Physics* **152, p** 481, 1994.

[5] Ballester J L, Oliver R, and Carbonell M, *Astronomy and Astrophysics* **431,** p 5, 2005.

[6] Chang H Y, *New Astronomy* **13.** p 185, 2008.

[7] Li K J *et al Journal of Geophysal Research Space Physics* **114,** p 4, 2009.

[8] El-Borie M A, El-Taher A M, Thabet A A, Ibrahim S F, Aly N S, and Bishara A A, *Astrophysical Journal* **898,** p 73, 2020.

[9] Joshi A, *Solar Physics* **157,** p 315, 1995.

[10] Bai T, *Astrophysical Journal Letters* **364**, p L17, 1990.

[11] Joshi B and Pant P, *Astronomy and Astrophysics* **431,** p 359, 2005.

[12] Ataç T and Özgüç A, *Solar Physics* **166,** p 201, 1996.

[13] Temmer M., Veronig A., Hanslmeier A., Otruba W., and Messerotti M, *Astronomy and Astrophysics* **375.** p 104, 2001.

[14] Joshi N. C., Bankoti N. S., Pande S., Pande B., and Pandey K, *Solar Physics* **260,** p 451, 2009.

[15] Vizoso G and Ballester J L, *Solar Physics* **112,** p 315, 1987.

[16] Gao P X, Li Q X, and Zhong S H, *Journal of Astrophysics and Astronomy* **28,** (2007)

[17] Veronig A, Temmer M, Hanslmeier A, Otruba W, and Messerotti M, *Astronomy and Astrophysics* **382,** p 1070, 2002.

[18] Joshi B and Joshi A, *Solar Physics* **219,** p 343, 2004.

[19] Nair S. and Prabhakaran Nayar S R, *Indian Journal of Radio & Space Physics* **37,** p 391, 2008.

[20] El-Borie M A, *IL NUOVO CIMENTO* **24 C,** p 6, 2001.

[21] El-Borie M A, El-Taher A M, Aly N E, and Bishara A A, *Physics of Plasmas* **25,** p 042901, 2018.

[22] El-Borie M A, El-Taher A M, Aly N E, and Bishara A A, *Astrophysics and Space Science* **363,** p 5, 2018.

[23] El-Borie M A, El-Taher A M, Aly N E, and Bishara A A, *Astroparticle Physics* **100,** p 13, 2018.

[24] El-Borie M A, El-Taher A M, Aly N E, and Bishara A A, *Solar Physics* **295,** p 122, 2020.

[25] Howard R, *Solar Physics* **38,** 1974.

[26] Temmer M *et al Astronomy and Astrophysics* **447,** p 735, 2006.

[27] El-Borie M A, El-Taher A M, Aly N E, and Bishara A A, *Astrophysical Journal* **880,** p 9, 2019.

[28] Prabhakaran Nayar S R, Radhika V N, Revathy K, and Ramadas V, *Solar Physics* **208,** p 359, 2002.

[29] Bazilevskaya G A *et al* Journal *of Physics: Conference Series* **632,** p 12050, 2015.

[30] Kupriyanova E. G., Melnikov V. F., Nakariakov V. M., and Shibasaki K, *Solar Physics* **267,** p 329, 2010.

[31] Chowdhury P, Gokhale M H, Singh J, and Moon Y-J, *Astrophysics and Space Science*, **361,** p 54, 2016.

[32] Chowdhury P, Kilcik *A*, Yurchyshyn V, Obridko V N, and Rozelot J P, *Solar Physics*, **294,** p 54, 2019.

[33] Thabet A A and El-Taher A M *Indian Journal of Physics* **1**, 2021.

[34] Daubechies I, *IEEE Transactions on Information Theory* **36,** p 961, 1990.

[35] Kumar P and Foufoula-Georgiou E, *Reviews of Geophysics* **35,** p 385, 1997.

[36] Torrence C and Compo G P, *Bulletin of the American Meteorological Society* **79,** p 61, 1998.

[37] Ippolitov I I, Kabanov M V, and Loginov S V, *Russian Physics Journal* **45** 1086 (2002)

[38] Valdés-Galicia J F and Mendoza B, *Solar Physics* **178,** p 183, 1998.

[39] Kato C, Munakata K, Yasue S, Inoue K, and McDonald F B, *Journal of Geophysical Research: Space Physics* **108,** p A10, 2003.

[40] Lean J L and Brueckner E G, *Astrophysical Journal* **337,** p 568, 1989.

[41] Hill M E, Hamilton D C, and Krimigis S M, *Journal of Geophysical Research* **106,** p 8315, 2001.

[42] Cane H v, Richardson I G, and von Rosenvinge T T, *Geophysical Research Letters* **25**, p 4437, 1998.

[43] Mursula K, Hiltula T, and Zieger B, *Geophysical Research Letters* **29,** p 15, 2002.

[44] Katsavrias Ch, Preka-Papadema P, and Moussas X, *Solar Physics* **280,** p 623, 2012.

[45] El-Borie M A, *Solar Physics* **208,** p 345, 2002.